

## NOTE

The  $b^1\Sigma_g^+ - X^3\Sigma_g^-$  (3, 0) Band of  $^{16}\text{O}_2$  and  $^{18}\text{O}_2$ 

The  $b^1\Sigma_g^+ - X^3\Sigma_g^-$  red atmospheric system of the  $\text{O}_2$  molecule is, despite its small oscillator strength, of importance for light scattering and extinction studies of the Earth's atmosphere. For this reason, this band system has, after the pivotal study of Babcock and Herzberg (1), been subjected to numerous investigations aimed at the determination of line positions, intensities (2), and pressure-induced effects. Since the potential curves of the  $b^1\Sigma_g^+$  excited and the  $X^3\Sigma_g^-$  ground electronic states are similar in shape, the intensity is mainly diagonal ( $\Delta v = 0$ ) and the off-diagonal Franck-Condon factors rapidly decrease. The (3, 0) band near 590 nm, which is  $10^4$  times weaker than the (0, 0) band, was recently investigated in the laboratory by Biennier and Campargue (3) using the sensitive method of intracavity laser absorption spectroscopy.

In a program to determine accurate line positions for various oxygen isotopes in the  $b-X$  system (4, 5), we present a high-resolution study of the (3, 0) band for  $^{16}\text{O}_2$  and  $^{18}\text{O}_2$ . In our experiment, we employ the method of cavity-ring-down spectroscopy (CDRS), which was recently reviewed (6). For details of the experimental setup we refer to this review and to our previous studies on the (0, 0) and (1, 0) bands (4, 5). A relevant detail is the use of mirrors for the optical cavity, with reflectivities of  $R \geq 99.99\%$  in the wavelength range of the (3, 0) band. In the experiment, we achieved a noise equivalent detection limit of  $1.0 \times 10^{-9} \text{ cm}^{-1}$ , which allowed us to record spectra of the (3, 0) band. Examples of spectra are shown in Fig. 1 for  $^{16}\text{O}_2$  and in Fig. 2 for  $^{18}\text{O}_2$ . The intensities of the individual lines are on the order of  $20 \times 10^{-9} \text{ cm}^{-1}$  at typical pressures of 200 Torr. The experiment involved a scanning pulsed laser with stepsize  $0.01 \text{ cm}^{-1}$ ; for data acquisition we averaged over five laser pulses at each position. For the recording of  $^{18}\text{O}_2$  spectra, a 95% enriched  $^{18}\text{O}_2$  sample (Eurisotop) was used.

For the purpose of wavelength calibration, we simultaneously recorded an  $\text{I}_2$ -absorption spectrum. By elementary methods of computerized curve fitting, interpolation, linearization, and comparison with the values from the  $\text{I}_2$  atlas (7), including a recalibration of the atlas involving a shift of  $-0.0056 \text{ cm}^{-1}$  (8), the positions of the oxygen resonances were determined. In some cases, e.g., for the  $^R R(11)$  and  $^R R(15)$  lines of  $^{18}\text{O}_2$ , a two-component fit was performed to deconvolute the line positions of partially overlapped lines. In the region of the  $P$  branches of  $^{18}\text{O}_2$ , some additional lines were observed that could be assigned as water vapor lines. The results of the line fitting and calibration procedures are presented in Table 1 for  $^{16}\text{O}_2$  and in Table 2 for  $^{18}\text{O}_2$ . The data pertaining to  $^{18}\text{O}_2$  follow from a single recording, while the ones for  $^{16}\text{O}_2$  are the result of an average over two recordings.

In a spectroscopic analysis of the data, the effective Hamiltonian of Rouillé *et al.* (9) was used to describe the  $X^3\Sigma_g^-$  ground state. Since the molecular constants for  $X^3\Sigma_g^-$ ,  $v = 0$  are very accurately known from far-infrared and microwave spectroscopy (for  $^{16}\text{O}_2$ , see Ref. (9), and for  $^{18}\text{O}_2$ , see Ref. (10)), the molecular constants were kept fixed at the values listed in our previous study on the (0, 0) band (4). It is noted that the zero-point energy is taken at the trace of the Hamiltonian for the ground state, so this value does not coincide with a particular quantum state. For the  $b^1\Sigma_g^+$ ,  $v = 3$  excited state we use the representation

$$E(N) = \nu_{30} + B_3 N(N+1) - D_3 N^2(N+1)^2. \quad [1]$$

All data of Tables 1 and 2 were incorporated in least-squares fitting routines

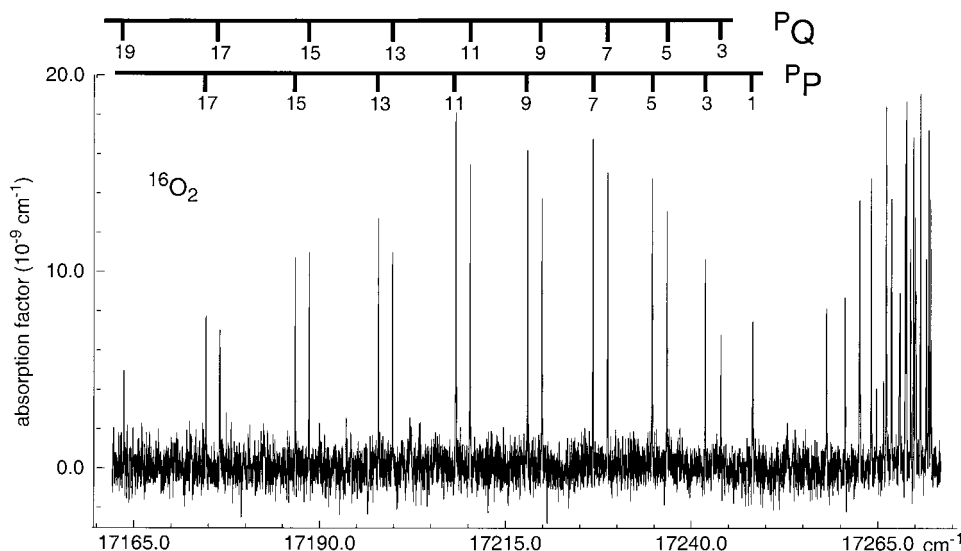


**FIG. 1.** Cavity-ring-down spectral recording of the  $b^1\Sigma_g^+ - X^3\Sigma_g^-$  (3, 0) band of  $^{16}\text{O}_2$  at a pressure of 183 Torr. The baseline was corrected for the loss rate related to the limited mirror reflectivity. For the  $P$  branches an assignment is given.

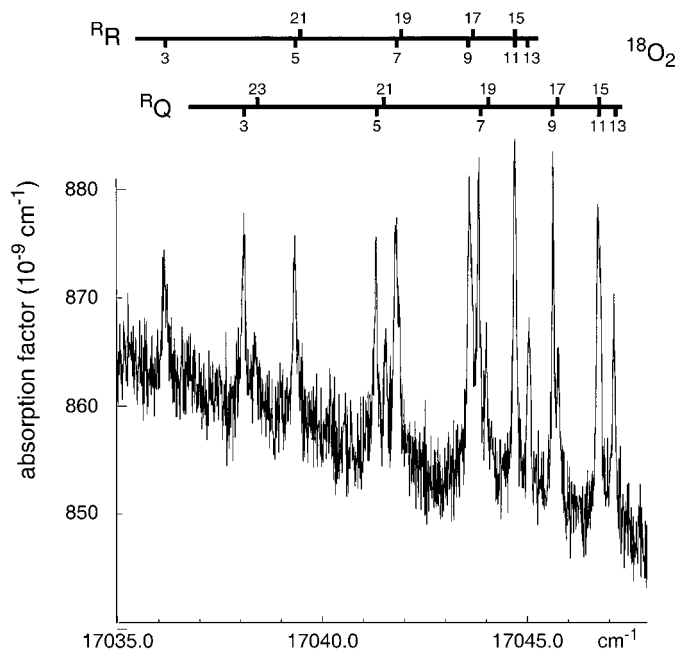


FIG. 2. Spectrum of the  $R$  branches of the  $b^1\Sigma_g^+ - X^3\Sigma_g^-$  (3, 0) band of  $^{18}\text{O}_2$  recorded at a pressure of 223 Torr. The varying baseline represents the variation in mirror reflectivity in this wavelength range.

yielding values and uncertainties ( $1\sigma$ ) for the  $\nu_3$ ,  $B_3$ , and  $D_3$  molecular constants, which are listed in Table 3. In the table, a comparison is made with previous values obtained for  $^{16}\text{O}_2$ ; the data of Babcock and Herzberg

( $J$ ) were reanalyzed in Ref. (3). The uncertainties in the experimental data were taken such that the least-squares fits converge with  $\chi^2$  values of 1.0 per data point. This is achieved by setting the uncertainty at  $0.007\text{ cm}^{-1}$  for the data of  $^{16}\text{O}_2$  and  $0.015\text{ cm}^{-1}$  for the data of  $^{18}\text{O}_2$ . The resulting values for the rotational constants  $B_3$  and  $D_3$  agree well with those of Biennier and Campargue (3), the present ones being more accurate. This improvement may be explained by the narrower linewidths of  $0.07\text{ cm}^{-1}$  in the present study compared to  $0.14\text{ cm}^{-1}$  in Ref. (3); a small discrepancy may be related to the difference in pressure broadening in both experiments. Both laboratory studies, the present CDRS study and the ICLAS study (3), have superior accuracy over the old data of Babcock and Herzberg ( $J$ ). Constants for  $^{18}\text{O}_2$  were not determined previously.

For a comparison of the band origins  $\nu_{30}$ , pressure-induced shifts have to be considered. In the present study, pressures of 183 Torr ( $^{16}\text{O}_2$ ) and 223 Torr ( $^{18}\text{O}_2$ ) of pure oxygen were used for the spectral recordings. We note that the values for  $\nu_{30}$  in Table 3 are not corrected for these pressure shifts. The spectra of Babcock and Herzberg ( $J$ ) were recorded through a large air mass, where the absorption is integrated over a range of altitude-dependent pressures, the dominant contribution originating from ambient atmospheric conditions. The ICLAS data (3) were recorded with a cell filled with 600 Torr pure oxygen, surrounded by ambient air, conditions for which a similar pressure shift as in Ref. ( $J$ ) was expected. Biennier and Campargue have commented that the data of Ref. ( $J$ ) may possess a systematic measurement shift of  $0.02\text{ cm}^{-1}$ . We find, from a study at lower pressure, a value for  $\nu_{30}$  which is smaller by  $0.012 \pm 0.005\text{ cm}^{-1}$  compared to Ref. (3). Phillips and Hamilton ( $II$ ) have determined  $\text{O}_2$  self-broadening pressure shifts amounting to  $-0.011\text{ cm}^{-1}\text{ atm}^{-1}$  for the (0, 0) band and  $-0.014\text{ cm}^{-1}\text{ atm}^{-1}$  for the (1, 0) band. In a simple extrapolation, a pressure shift of  $-0.02\text{ cm}^{-1}\text{ atm}^{-1}$  would follow for the (3, 0) band. Such an assumption would bring the present value in accordance with the value of Ref. ( $J$ ) rather than that of Ref. (3). A final resolution of this issue will await measurement of pressure shifts in the (3, 0) band, including shifts induced by  $\text{N}_2$ .

The present data allow for a determination of the absorption strength of the

TABLE 1  
The  $b^1\Sigma_g^+ - X^3\Sigma_g^-$  (3, 0) Band of  $^{16}\text{O}_2$

N	$P_Q$		$P_P$		$R_R$		$R_Q$	
	observed	$\Delta_{o-c}$	observed	$\Delta_{o-c}$	observed	$\Delta_{o-c}$	observed	$\Delta_{o-c}$
1			17248.241	-0.004			17258.136	-0.002
3	17243.972	0.002	17241.887	0.002	17260.592	0.003	17262.541	0.003
5	17236.723	-0.003	17234.713	-0.001	17264.100	-0.001	17266.086	-0.003
7	17228.704	-0.002	17226.743	0.010	17266.798	0.001	17268.807	-0.006
9	17219.880	-0.006	17217.934	-0.006	17268.673	-0.002	17270.705	-0.009
11	17210.268	0.009	17208.349	0.012	17269.731	-0.001	17271.796	0.003
13	17199.825	0.001	17197.922	-0.002	17269.969	0.003	17272.053	0.005
15	17188.582	0.003	17186.697	-0.002	17269.365	-0.011	17271.482	0.005
17	17176.533	0.009	17174.673	0.010	17267.950	-0.007	17270.080	0.002
19	17163.666	0.009	17161.804	-0.011	17265.715	0.006	17267.841	-0.007
21	17149.966	-0.011	17148.138	-0.015	17262.626	0.000	17264.799	0.016

(a) values in  $\text{cm}^{-1}$

TABLE 2  
The  $b^1\Sigma_g^+ - X^3\Sigma_g^-$  (3, 0) Band of  $^{18}\text{O}_2$

N	$P_Q$		$P_P$		$R_R$		$R_Q$	
	observed	$\Delta_{o-c}$	observed	$\Delta_{o-c}$	observed	$\Delta_{o-c}$	observed	$\Delta_{o-c}$
1			17025.088	-0.003	17032.275	0.040	17034.148	0.004
3	17021.505	-0.003	17019.464	0.009	17036.146	0.023	17038.070	-0.017
5	17015.118	-0.001	17013.115	-0.007	17039.305	-0.005	17041.278	-0.027
7	17008.051	-0.006	17006.086	-0.004	17041.768	-0.027	17043.806	-0.007
9	17000.334	0.029	16998.370	0.009	17043.563	-0.013	17045.610	-0.005
11	16991.847	-0.012	16989.903	-0.033	17044.654	0.001	17046.719	0.009
13	16982.732	0.014	16980.818	0.005	17045.035	0.012	17047.084	-0.014
15	16972.890	0.009	16971.008	0.015	17044.699	0.013	17046.785	0.008
17	16962.355	0.009	16960.471	-0.004	17043.612	-0.026	17045.750	0.004
19	16951.124	0.009	16949.261	0.001	17041.880	0.002	17043.998	-0.004
21					17039.403	0.000	17041.519	-0.025
23							17038.382	0.014

(a) values in  $\text{cm}^{-1}$

(3, 0) band. Signal integration over all measured lines up to  $J = 21$  yields a value of  $9.3 \pm 0.4 \cdot 10^{-27}$  cm/molecule. However, this value needs correction for the effect of laser bandwidth. If we take the bandwidth of the laser to  $0.05 \text{ cm}^{-1}$ , then this value coincides with the combined effects of Doppler and collisional broadening. Since Doppler broadening dominates, we deconvolute the absorption strength by using Gaussian profiles, leading to a correction factor of 1.41. Hence, a band intensity of  $1.3 \pm 0.1 \cdot 10^{-26}$  cm/molecule is obtained for the (3, 0) band of the  $^{16}\text{O}_2$  isotopomer. This value is somewhat smaller than the one obtained in Ref. (3). When comparing with the band intensity of the (2, 0) band (12), we find that the (3, 0) band is 35 times weaker

than the (2, 0) band, in accordance with calculated Franck–Condon factors (13). Following a similar procedure, we derive a band intensity of  $1.6 \pm 0.1 \cdot 10^{-26}$  cm/molecule for the (3, 0) band of the  $^{18}\text{O}_2$  isotopomer. From the fact that the  $v = 3$  wavefunction lies lower in the  $b^1\Sigma_g^+$  potential, a larger overlap with the  $X^3\Sigma_g^-$ ,  $v = 0$  wavefunction may be expected, and hence, a larger band intensity.

Our study yields updated or new values for the molecular constants for the  $b^1\Sigma_g^+ - X^3\Sigma_g^-$  (3, 0) band of  $^{16}\text{O}_2$  and  $^{18}\text{O}_2$ . These values may help to identify emission bands from excited vibrational levels of  $\text{O}_2(b^1\Sigma_g^+)$ , including minority isotopomers, as observed in the Earth's atmosphere (14, 15).

TABLE 3  
Molecular Constants for the  $b^1\Sigma_g^+$ ,  $v = 3$  Excited State of Molecular Oxygen

	$^{16}\text{O}_2$ (this work)	$^{16}\text{O}_2$ (ref. [1])	$^{16}\text{O}_2$ (ref. [5])	$^{18}\text{O}_2$ (this work)
$\nu_{30}$	17252.452 (3)	17252.428 (8)	17252.464 (4)	17028.978 (4)
$B_3$	1.33611 (3)	1.33626 (51)	1.33614 (26)	1.19063 (5)
$D_3$	$5.43 (5) \cdot 10^{-6}$	$5.63 (47) \cdot 10^{-6}$	$5.54 (22) \cdot 10^{-6}$	$4.23 (9) \cdot 10^{-6}$

The values for  $\nu_{30}$  are not corrected for possible pressure shifts (see text). The values in the second column are the ones derived in a reanalysis of the data of ref. [1] performed by the authors of ref. [5]. All values in  $\text{cm}^{-1}$ .

## ACKNOWLEDGMENTS

The authors thank H. Hoppe (University of Konstanz) for contributing to the measurements and acknowledge financial support from the Space Research Organization Netherlands (SRON).

## REFERENCES

1. H. B. Babcock and L. Herzberg, *Astrophys. J.* **108**, 167–190 (1948).
2. V. D. Galkin, *Opt. Spectrosc.* **47**, 151–153 (1979).
3. L. Biennier and A. Campargue, *J. Mol. Spectrosc.* **188**, 248–250 (1998).
4. H. Naus, A. de Lange, and W. Ubachs, *Phys. Rev. A* **56**, 4755–4763 (1997).
5. H. Naus, S. J. van der Wiel, and W. Ubachs, *J. Mol. Spectrosc.* **192**, 162–168 (1998).
6. M. D. Wheeler, S. N. Newman, A. J. Orr-Ewing, and M. Ashfold, *J. Chem. Soc., Faraday Trans.* **94**, 337–352 (1998).
7. S. Gerstenkorn and P. Luc, "Atlas du Spectre d'Absorption de la Molecule de l'Iode Entre 14 800–20 000  $\text{cm}^{-1}$ ", Ed. Presses du CNRS, Paris, 1978.
8. S. Gerstenkorn and P. Luc, *Rev. Phys. Appl.* **8**, 791–794 (1979).
9. G. Rouillé, G. Millot, R. Saint-Loup, and H. Berger, *J. Mol. Spectrosc.* **154**, 372–382 (1992).
10. W. Steinbach and W. Gordy, *Phys. Rev. A* **11**, 729–731 (1975).
11. A. J. Phillips and P. A. Hamilton, *J. Mol. Spectrosc.* **174**, 587–594 (1995).
12. L. S. Rothman, R. R. Gamache, R. H. Tipping, C. P. Rinsland, M. A. H. Smith, D. C. Benner, J. Malathy-Devi, J.-M. Flaud, C. Camy-Peret, A. Perrin, A. Goldman, S. T. Massie, L. R. Brown, and R. A. Toth, *J. Quant. Spectrosc. Radiat. Transfer* **48**, 469–507 (1992).
13. D. L. Albritton, W. J. Harrop, A. L. Schmeltekopf, and R. N. Zare, *J. Mol. Spectrosc.* **46**, 103–108 (1973).
14. D. E. Osterbrock, J. P. Fulbright, A. R. Martel, M. J. Keane, S. C. Trager, and G. Basri, *Astron. Soc. of the Pacific*, **108**, 277–308 (1996).
15. T. G. Slinger, D. L. Huestis, D. E. Osterbrock, and J. P. Fulbright, *Science* **277**, 1485–1488 (1997).

H. Naus  
W. Ubachs

*Department of Physics and Astronomy  
Vrije Universiteit  
De Boelelaan 1081  
1081 HV Amsterdam  
The Netherlands*

*Received September 9, 1998; in revised form October 10, 1998*